Adaptive Driving Situation Characterization for Predicting the Driving Load of Electric Vehicles in Uncertain Environments

Javier A. Oliva[1], Torsten Bertram[2]

[1,2] *Institute of Control Theory and Systems Engineering, Technische Universität Dortmund, Germany*
javier.oliva@tu-dortmund.de
torsten.bertram@tu-dortmund.de

ABSTRACT

Battery powered electric vehicles (EVs) have emerged as a promising solution for reducing the consumption of fossil fuels in modern transportation systems. Unfortunately the battery pack has a low energy storage capacity, which causes the driving range of the EV to become very limited. It is therefore essential to properly characterize the different driving situations of the vehicle in order to better predict the driving load along the road ahead and to better estimate the remaining driving range (RDR). However, this prediction cannot be achieved straightforward due to sources of uncertainty introduced by the randomness of the driving environment. In this paper a novel approach for characterizing driving situations and for predicting the driving load of an EV is presented. The prediction of the driving load occurs in a model-based fashion, where the model input variables are modeled as discrete-time Markov processes. An approach for estimating the transition probabilities between Markov states in the presence of sparse driving data is introduced. Furthermore, to capture the changes in the driving environment a Bayes-based methodology for recursively updating the established transition probabilities is presented. The validity of the proposed approach is illustrated through simulation and by a series of experimental case studies.

1. INTRODUCTION

In modern times, the use of battery powered electric vehicles (EVs) has grown due to they offer a promising solution for reducing the consumption of fossil fuels. However, the limited energy storage capacity of the battery pack causes the driving range of the EV to become very limited. A proper characterization of driving situations is therefore essential in order to better predict the driving load, i.e., the electrical power demanded to propel the EV along the road ahead. Such a prediction can be used, for example, by an advanced driver assistance system (ADAS) to estimate the RDR of the EV in a more accurate manner. However, this prediction cannot be achieved straightforward due to many sources of uncertainty introduced by the randomness of the driving environment. Key affecting factors such as the road profile, the driving style or the traffic conditions are highly uncertain and are usually difficult to predict.

To the best of our knowledge, few studies have addressed the problem of predicting the driving load in EVs. (Wang, Xu, Li, & Xu, 2007) combine cascade neural networks with a node-decoupled extended Kalman filter to forecast the driving load. In this work the authors define five load levels by fuzzy logic and, instead of predicting an entire sequence of loads, the load level is forecast. In (Yang, Huang, Tan, & He, 2008) the driving load of a hybrid electric vehicle (HEV) is predicted by using the discrete cosine transform (DCT) together with support vector machines (SVM). Similar to the approach previously mentioned, the authors classifie the driving load into five predefined levels. The forecasting task deals with the decision about the next load level. An approach that predicts the battery power requirements for EVs in real time by combining road information from a static map with historical driving data is introduced by (Kim, Lee, & Shin, 2013).

The drawback with the aforementioned approaches is that none of them treat the driving load in a stochastic manner. As it has been shown in (Oliva, Weihrauch, & Bertram, 2013), estimating the RDR of an EV requires characterizing the uncertainty introduced by driving environment. Because of this, this contribution deals with a novel approach for characterizing driving situations and with an algorithm for predicting the driving load of an EV. The prediction of the driving load takes place under a model-based approach. A model of the powertrain of an EV is used to compute the electrical power demand of the electric motor as response to the road properties, the vehicle speed and the acceleration, which in this paper constitute the input variables of the model. The evolution of the input variables in time is first modeled as a homogeneous discrete-time Markov process. An offline approach for

estimating the transition probabilities between states in the presence of sparse data is introduced. This allows completely characterizing the uncertainty in the transition probabilities of the Markov state space even if information about some transitions between states is unavailable. However, relying solely on the Markov transition models identified offline for predicting the driving load usually does not adequately describe the most recent driving situation. For this reason we also present a Bayes-based methodology for updating the transition probabilities as new information about the driving situation becomes available.

The remainder of this paper is organized as follows: Section 2 deals with the physical model of an EV used to compute the driving load. In section 3 the characterization of driving situations is discussed and two offline methods for estimating the transition probabilities between Markov states are introduced. Section 4 explains the steps needed for updating the transition probabilities on receipt of new information about the driving situation. In section 5 the algorithm used for predicting the driving load is described. Section 6 presents the simulation and experimental results used for validating the proposed approach. Finally, section 7 concludes the findings of this work and provides an outlook on our future work.

2. DRIVING LOAD MODELING IN EVS

As it was already mentioned, the prediction of the driving load is carried out in a model-based fashion. From a physical point of view, the driving load can be either modeled by a forward-facing or by a backward-facing approach (Guzzella & Sciarretta, 2005). In the forward-facing approach the EV is controlled to follow a desired speed. This approach considers the physical properties of each component of the powertrain and the dynamic interaction between them. The drawback with this modeling approach is the high computational burden required to solve the set of differential equations presented in the model. This paper employs the backward-facing approach, for modeling the driving load of the EV. The backward-facing approach is computationally efficient since it assumes that the EV moves exactly with an imposed speed. The model calculates the forces acting on the wheels and processes them backwards through the powertrain. The computation of the power demand depends only on algebraic equations, decreasing in this manner the computational effort of the model. Fig. 1 depicts the structure of the model used to compute the driving load. As it is explained in the following two sections, the input $\mathbf{u}$ is given by the speed v and acceleration a of the vehicle and by the inclination (slope) θ of the road. The output y of the model is the electrical power demanded by the electric motor, denoted here as P_{ele}.

The following section explains the model in detail. We omit expressing the variables of the model as time dependent, since this model is described by a set of algebraic equations.

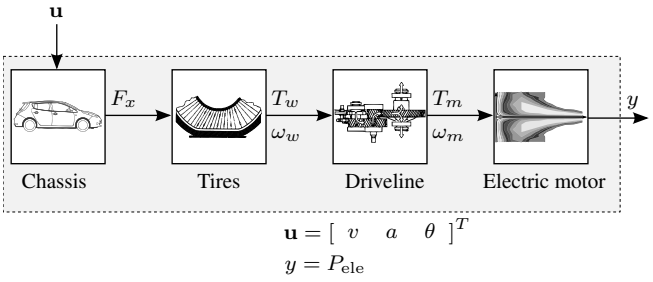

Figure 1. Structure of the backward-facing approach for modeling the driving load of an EV.

2.1. Backward-facing Approach

An electric vehicle is composed by many components which, for simplification purposes, can be considered to move uniformly. As shown in Fig. 2, the force F_x required to propel the vehicle forward can be computed by

$$F_x = F_{air} + F_g + F_r + F_i, \tag{1}$$

where:

- $F_{air} = \frac{1}{2}\rho_{air} c_w A v^2$ is the aerodynamic drag force,
- $F_g = mg\sin(\theta)$ is the hill climbing force,
- $F_r = mgK_r$ is the rolling resistance and
- $F_i = ma$ is the force needed to accelerate/decelerate the vehicle.

The parameter ρ_{air} is the density of air, c_w is the aerodynamic drag coefficient, A and m are the frontal area and the mass of the vehicle, g is the gravitational acceleration and K_r is the rolling resistance coefficient.

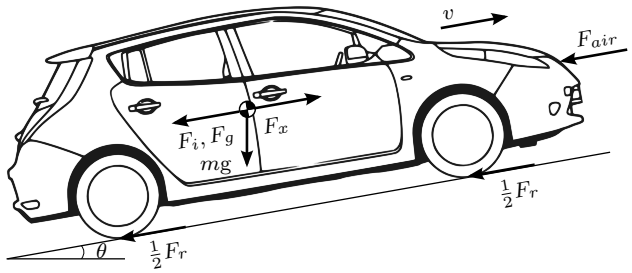

Figure 2. Forces acting during the motion of an EV.

The mechanical power P_{mec} demanded by the electric motor is easily calculated by means of a polynomial power requirement model as follows:

$$P_{mec} = F_x v = \frac{1}{2}\rho_{air} c_w A v^3 + mg\sin(\theta)\, v + mgK_r v + mav. \tag{2}$$

As suggested by (Guzzella & Sciarretta, 2005), the relationship between the mechanical and the electrical power demand

of an electric motor can be computed, with a certain degree of accuracy, by employing a stationary map of the electric motor's efficiency as a function of the rotor's rotational speed and the torque demand

$$P_{ele} = \frac{P_{mec}}{\eta_m\left(\omega_m, T_m\right)}, P_{mec} > 0. \tag{3}$$

In Eq. (3) the electric motor's efficiency is represented by η_m , $\omega_m = \frac{v i_d}{r_{tire}}$ is the rotational speed of the rotor and $T_m = \frac{F_x r_{tire}}{i_d}$ is the torque demand of the motor. Here r_{tire} and i_d are the tire's radius and the gear ratio of the driveline respectively.

One important feature of modern EVs is that certain amount of the kinetic and the potential energy can be recovered by means of the regenerative braking system. During braking maneuvers the electric motor is operated as a generator, providing in this manner an extra braking torque to the wheels. The recovered energy can then be used to supply power either to the powertrain or to the auxiliary accessories. The amount of braking torque depends on the operation strategy of the braking system. The operation strategy optimizes the distribution of braking torque between the mechanical and the regenerative brakes in such a way, that the maximum electrical power is generated. The electrical power generated is computed by

$$P_{ele} = P_{mec}\eta_m\left(\omega_m, -T_m\right) k_{v_x}, P_{mec} < 0. \tag{4}$$

Since the generated power depends on ω_m, it would be a difficult task to supply power to the power bus at low speeds. Because of this the parameter k_{v_x} is used to limit the usage of the electric motor in generator mode according to Eq. (5), so that the mechanical brakes are applied at very low speeds and at high speeds the vehicle is braked mostly by the electric motor.

$$k_{v_x} = \begin{cases} 0 & v_x \leq 3.5 \text{ m/s} \\ \frac{v_x - 3.5}{5} & 3.5 < v_x < 8 \text{ m/s} \\ 0.9 & v_x \geq 8 \text{ m/s} \end{cases} \tag{5}$$

The efficiency map η_m is usually well defined just for the motor mode (upper quadrant of Fig. 3). In order to extend the map to the generator mode, the power losses are mirrored as follows

$$\eta_m\left(\omega_m, -T_m\right) = 2 - \frac{1}{\eta_m\left(\omega_m, T_m\right)}. \tag{6}$$

Even though the computed efficiency map obtained by applying Eq. (6) slightly differs from the data that can be obtained by measuring the efficiency of the electric motor working as generator, it offers a practical and accurate solution for modeling the electric motor also in generator mode.

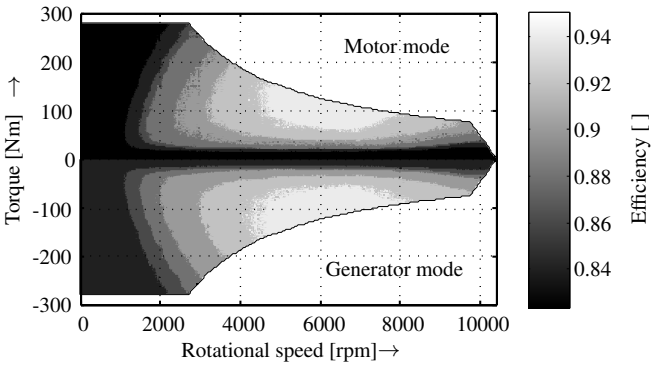

Figure 3. Efficiency map of an electric motor.

2.2. Factors Affecting the Prediction of the Driving Load

To properly predict the driving load under a model-based approach it is necessary to analyze the dynamics of each of the parameters of Eq. (2) and to determine the source of information needed to acquire them, in order to differentiate between time invariant and time variant model parameters, from now on referred as *constants* and *input variables*, respectively. On the one hand, input variables are characterized by their high dynamic and are usually easily measurable. On the other hand, the constants, as the term suggests, rarely change or change very slowly. Table 1 summarizes the dynamics and presents the sources of information required to acquire each of the parameters involved in the computation of P_{mec}.

Parameter	Dynamics	Source of information
a $\left(\mathrm{m/s^2}\right)$	Very high	Driver, road, traffic
v $\left(\mathrm{m/s}\right)$	High	Driver, road, traffic
m $\left(\mathrm{kg}\right)$	Nearly constant	Vehicle design
g $\left(\mathrm{m/s^2}\right)$	Nearly constant	Altitude
K_r	High	Road
θ $(^\circ)$	High	Road
ρ_{air} $\left(\mathrm{kg/m^3}\right)$	Low	Altitude
c_w	Nearly constant	Vehicle design
A $\left(\mathrm{m^2}\right)$	Nearly constant	Vehicle design

Table 1. Dynamics and sources of information required for the acquisition of the parameters affecting the prediction of the driving load.

The parameters g and ρ_{air}, even though they can be easily determined, depend on the altitude and rarely change during a trip. Also m, c_w and A can be easily acquired. They don't change since they depend on the vehicle design. The friction coefficient K_r, despite its high dynamics, cannot be measured, and therefore it has to be either assumed or estimated. For this reason we consider it as a constant parameter under the assumption that the road conditions do not change drastically during a trip.

The slope θ changes rapidly according to the road type and can be easily acquired either by integrating a GPS into the EV or by using a navigation system with a preloaded static GIS

(Geographic Information System). The speed v and the acceleration a depend on many factors that are difficult to predict and that exhibit some degree of randomness. To these factors belong the road type, the traffic conditions or the driver aggressiveness, just to name a few. Hence v and a change very dynamically and have to be treated as time variant.

The parameters v, a and θ are considered in this work as the model input variables, since they meet the requirements previously mentioned. Accordingly, the input vector, used here to denote a driving situation, is given by

$$\mathbf{u} = \begin{bmatrix} v & a & \theta \end{bmatrix}^T. \tag{7}$$

The characterization of the input variables is explained in detail in the following section.

3. DRIVING SITUATION CHARACTERIZATION

By assuming that the input vector $\mathbf{u} = \begin{bmatrix} v & a & \theta \end{bmatrix}^T$ evolve in time following a discrete-time stochastic process $\{\mathbf{u}_k\}$ and that it can take on values in a countable set $\boldsymbol{\mathcal{U}}$, called the state space, then its behavior can be successfully modeled as a first order Markov chain, under the assumption that it satisfies the so called Markov property. This property states that, the future state $\mathbf{u}_{k+1}$ depends only on the current state $\mathbf{u}_k$ and not on all previous states $\mathbf{u}_0, \mathbf{u}_2, \ldots, \mathbf{u}_{k-1}$. In other words, for all $\{\mathbf{u}_k, k \geq 0\}$

$$\begin{aligned} \pi_{i,j} &= p\left(\mathbf{u}_{k+1} = j | \mathbf{u}_k = i, \mathbf{u}_{k-1}, \ldots, \mathbf{u}_0\right) \\ &= p\left(\mathbf{u}_{k+1} = j | \mathbf{u}_k = i\right), \end{aligned} \tag{8}$$

where $\pi_{i,j}$ is known as conditional transition probability and k denotes the discrete time step. All transition probabilities between states are grouped in a transition probability matrix $\boldsymbol{\Phi}$ of the form

$$\boldsymbol{\Phi} = \begin{bmatrix} \pi_{1,1} & \pi_{1,2} & \cdots & \pi_{1,m} \\ \pi_{2,1} & \pi_{2,2} & \cdots & \pi_{2,m} \\ \vdots & \vdots & \ddots & \vdots \\ \pi_{m,1} & \pi_{m,2} & \cdots & \pi_{m,m} \end{bmatrix}. \tag{9}$$

Then, Eq. (8) can be expressed as

$$\pi_{i,j} = \boldsymbol{\Phi}\left(\mathbf{u}_{k+1} = j | \mathbf{u}_k = i\right), \tag{10}$$

where $\pi_{i,j}$ is the ij^{th} element of $\boldsymbol{\Phi}$. Since the elements j of $\boldsymbol{\Phi}$ represent the transition probabilities to all other states from i, each row satisfies the condition $\sum_{j=1}^{m} \pi_{i,j} = 1$ for all $j \in \boldsymbol{\mathcal{U}}$. Eq. (10) is said to be *time homogeneous* since $\pi_{i,j}$ is independent of k. To better estimate the transition probabilities of Eq. (10) the input state space is splitted up into $\mathbf{u}_k = \begin{bmatrix} \mathbf{u}_k^{va} & u_k^{\theta} \end{bmatrix}^T$, where $\mathbf{u}_k^{va} = \begin{bmatrix} v_k & a_k \end{bmatrix}$ and $u_k^{\theta} = \theta_k$ represent parts of the input state space given by the tuple (v, a) and by the slope θ, respectively. As shown in (Oliva et al., 2013), two transition probability matrices, namely $\boldsymbol{\Phi}^{va}$ and $\boldsymbol{\Phi}^{\theta}$ can be used to store all the information regarding the transition probabilities of the input variables. The following section introduces the methodology used in the estimation of the transition probabilities of both transition probability matrices (TPMs).

3.1. Characterization of $\boldsymbol{\Phi}^{va}$

In the presented approach, the structure of $\boldsymbol{\Phi}^{va}$ differs slightly from that of $\boldsymbol{\Phi}$ as it was introduced by Eq. (9). The states of the Markov chain are composed by $v_s \in \boldsymbol{\mathcal{V}}$ and by $a_i \in \boldsymbol{\mathcal{A}}$, where $\boldsymbol{\mathcal{V}}$ and $\boldsymbol{\mathcal{A}}$ represent the state space of the speed and acceleration of the EV. The definition of the conditional transition probability given by Eq. (10) is reformulated for this matrix as

$$\pi_{i,j}^{v_s a} = \boldsymbol{\Phi}^{v_s a}\left(a_{k+1} = j | a_k = i, v_k = s\right), \tag{11}$$

where $\pi_{i,j}^{v_s a}$ describes the probability of accelerating at rate a_j over the next time step given that the EV accelerates with a_i at given speed v_s in the current time step. The structure of $\boldsymbol{\Phi}^{va}$, with $\boldsymbol{\Phi}^{v_s a} \in \mathbb{R}^{\mathrm{M}\times\mathrm{M}}$ and $v_s \in \mathbb{R}^{\mathrm{N}}$, is shown in Fig. (4).

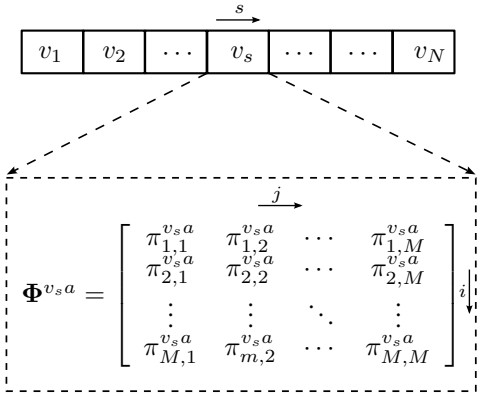

Figure 4. Structure of $\boldsymbol{\Phi}^{va}$.

The purpose of modeling $\mathbf{u}_k^{va}$ as a homogeneous Markov process is to describe the stationary distribution of speed and acceleration. In this work the transition probabilities of $\boldsymbol{\Phi}^{va}$ are estimated from historical driving data. Both a and v have to first be discretized. Accordingly, the state space is discretized as $\boldsymbol{\mathcal{A}} = \{a_{\min}, \ldots, -2a_{\text{res}}, -a_{\text{res}}, 0, a_{\text{res}}, 2a_{\text{res}}, \ldots, a_{\max}\}$ and by $\boldsymbol{\mathcal{V}} = \{0, v_{\text{res}}, 2v_{\text{res}}, \ldots, v_{\max}\}$, where $v_{\text{res}} = 1\ \text{km/h}$, $v_{\max} = 140\ \text{km/h}$, $a_{\text{res}} = 0.2\ \text{m/s}^2$, $a_{\min} = -3\ \text{m/s}^2$ and $a_{\max} = 3\ \text{m/s}^2$. The resolutions v_{res} and a_{res} offer a good trade-off between computational effort and accuracy.

3.1.1. Estimating the Stationary Distribution of $\boldsymbol{\Phi}^{va}$

In this work we use the maximum likelihood estimation (MLE) scheme (T. C. Lee, Judge, & Zellner, 1970) for estimating the time-invariant transition probabilities of $\boldsymbol{\Phi}^{va}$. A transition

probability $\pi_{i,j}^{v_s a}$ is computed by

$$\pi_{i,j}^{v_s a} = \frac{n_{i,j}}{n_i}, \tag{12}$$

where $n_{i,j}$ represents the number of times the EV changes its acceleration from a_i to a_j and n_i is the total number of times the EV accelerates with a_i at given speed v_s. This approach is very practical since the estimation can by achieved by simply *counting* the number of times a change in the acceleration occurs.

3.1.2. Approximating $\mathbf{\Phi}^{va}$ for unavailable data

As it will be shown in section 5, the construction of the Markov chain for a_k may lead to speed states v_s, computed by Eq. (29), where $\mathbf{\Phi}^{v_s a} \rightarrow \{0\}$, i.e., where no information about the distribution of the acceleration in the next time step is available. This is caused due to the sparsity of the historical driving data used for estimating the transition probabilities.

This issue can be sorted out by finding a suitable probability distribution function of the form $f(a_{k+1}|a_k = i, v_k = s)$ that can be employed for all $\mathbf{\Phi}^{v_s a} \rightarrow \{0\}$. The shape of such a function can be better understood by analyzing the distribution of a_{k+1} at different (v_k, a_k). One strong candidate for choosing f is the *Beta* distribution (Johannesson, Asbogard, & Egardt, 2007). Fig. 5 shows the Beta function fitted over different distributions of a_{k+1}.

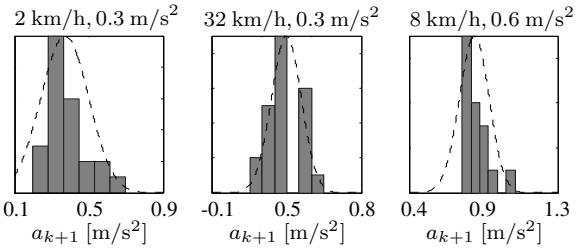

Figure 5. Fitted Beta function over the distribution of a_{k+1} at different (v_k, a_k).

The Beta density function is a versatile function which is usually employed for modeling different shapes of probability distributions, as shown in Fig. 6. The probability density function (PDF) of the generalized Beta distribution is given by

$$f\left(x|\alpha,\beta,b_L,b_U\right) = \frac{\left(x-b_L\right)^{\alpha-1}\left(b_U-x\right)^{\beta-1}}{\left(b_U-b_L\right)^{\alpha+\beta-1}}, \tag{13}$$

where α and β are the shape parameters of the Beta distribution and $[b_L, b_U]$ define the interval for which Eq. (13) is defined. The fact that the Beta PDF is defined just over a given interval can be exploited in that no accelerations beyond the admissible values, dictated by the performance of the EV, can be reached. Furthermore, b_L and b_U can be conveniently chosen to force any a_{k+1}, drawn from a Beta distribution given by Eq. (13), to lie within the bounds of the state space of $\mathbf{\Phi}^{v_s a}$, i.e., $a_{k+1} \in \boldsymbol{\mathcal{A}}$.

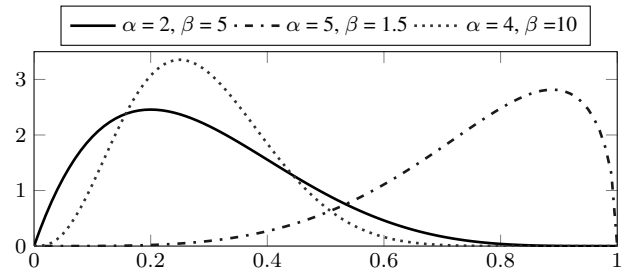

Figure 6. Different shapes of the Beta distribution on the interval with $b_L = 0$ and $b_U = 1$.

The first two moments of a_{k+1}, namely the expected value and the variance, are given by

$$E\left[a_{k+1}|\alpha,\beta,b_L,b_U\right] = b_L + \left(b_U - b_L\right)\frac{\alpha}{\alpha+\beta} \tag{14}$$

and

$$Var\left[a_{k+1}|\alpha,\beta,b_L,b_U\right] = \frac{\left(b_U-b_L\right)^2\alpha\beta}{\left(\alpha+\beta\right)^2\left(\alpha+\beta+1\right)}, \tag{15}$$

respectively. The function f can be reformulated in such a way that the parameters of the Beta distribution depend on the Markov states and that the PDF is defined only over the state space of a, i.e., $f\left(a_{k+1}|\alpha\left(a_k,v_k\right),\beta\left(a_k,v_k\right),a_{\min},a_{\max}\right)$. The task is then to estimate both α and β for the entire state space. To this aim we combine the Markov states of v and a and define a two-dimensional state space denoted by

$$\boldsymbol{\mathcal{S}} = \left\{a \in \mathbb{R}, v \in \mathbb{R} : \boldsymbol{\mathcal{A}}, \boldsymbol{\mathcal{V}}\right\}. \tag{16}$$

From the historical driving data we acquired all samples of a_{k+1} and store them in the correspondent state of $\boldsymbol{\mathcal{S}}$ according to the values of v_k and a_k. The purpose of the aforementioned step is to sort the historical data in such manner that both $E\left[a_{k+1}\right]$ and $Var\left[a_{k+1}\right]$ can be calculated with basic statistical operations from the available samples of a_{k+1}. Since the sparsity of the driving data causes $E\left[a_{k+1}\right]$ and $Var\left[a_{k+1}\right]$ to be defined pointwise over $\boldsymbol{\mathcal{S}}$, it is necessary to identify a function $g\left(a,v\right)$ and a function $h\left(a,v\right)$ that describe how $E\left[a_{k+1}\right]$ and $Var\left[a_{k+1}\right]$ vary throughout $\boldsymbol{\mathcal{S}}$, in order to completely parametrize the state space. This is accomplished by means of an approximation by bivariate tensor product B-Splines with a predefined sequence of knots (Johannesson, 2005). The sequence of knots is set denser where more information is available in order to better capture the behavior of the most important regions of $\boldsymbol{\mathcal{S}}$. The splines describing the variation of $E\left[a_{k+1}\right]$ and $Var\left[a_{k+1}\right]$, namely the functions $g\left(a,v\right)$ and $h\left(a,v\right)$, over $\boldsymbol{\mathcal{S}}$ are presented in Fig. 7 and in Fig. 8, respectively.

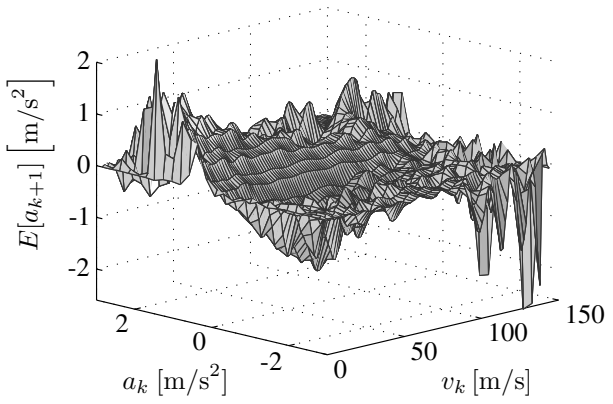

Figure 7. Function $g(a,v)$ representing the variation of $E[a_{k+1}]$ over $\boldsymbol{\mathcal{S}}$.

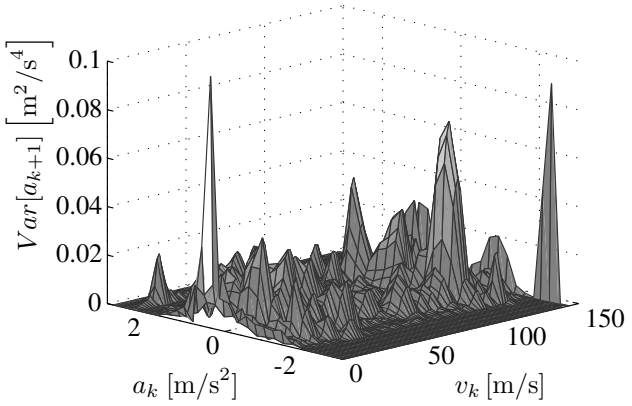

Figure 8. Function $h(a,v)$ representing the variation of $Var[a_{k+1}]$ over $\boldsymbol{\mathcal{S}}$.

Having identified $E[a_{k+1}]$ and $Var[a_{k+1}]$ for the entire state space, the parameters $\alpha(a,v), \beta(a,v)$ are estimated by moment matching, i.e., by evaluating $g(a,v)$ and $h(a,v)$ for each state on $\boldsymbol{\mathcal{S}}$ and by equating the result to the theoretical moments given by Eq. (14) and Eq. (15) (Abourizk, Halpin, & Wilson, 1994). Solving the obtained equation system for $\alpha(a,v)$ and $\beta(a,v)$ leads to

$$\alpha(a,v) = \frac{-(b_L-\mu)}{b_L-b_U} - \frac{(b_L-\mu)^2(b_U-\mu)}{\sigma^2(b_L-b_U)}, \tag{17}$$

$$\beta(a,v) = \frac{(b_U-\mu)}{b_L-b_U} + \frac{(b_L-\mu)(b_U-\mu)^2}{\sigma^2(b_L-b_U)} \tag{18}$$

where $\mu = E[a_{k+1}]$, $\sigma^2 = Var[a_{k+1}]$, $b_L = a_{\min}$ and $b_U = a_{\max}$.

3.2. Characterization of $\boldsymbol{\Phi}^{\theta}$

The transition probability matrix for the slope is given by

$$\boldsymbol{\Phi}^{\theta} = \begin{bmatrix} \pi^{\theta}_{1,1} & \pi^{\theta}_{1,2} & \cdots & \pi^{\theta}_{1,h} \\ \pi^{\theta}_{2,1} & \pi^{\theta}_{2,2} & \cdots & \pi^{\theta}_{2,h} \\ \vdots & \vdots & \ddots & \vdots \\ \pi^{\theta}_{h,1} & \pi^{\theta}_{h,2} & \cdots & \pi^{\theta}_{h,h} \end{bmatrix}. \tag{19}$$

The estimation of the transition probabilities of $\boldsymbol{\Phi}^{\theta}$ occurs similarly as shown in section 3.1.1 by applying the MLE to real road height profiles.

The state space of the Markov chain for the slope is given by $\boldsymbol{\Theta} = \{\theta_{\min}, \ldots, -2\theta_{\mathrm{res}}, -\theta_{\mathrm{res}}, 0, \theta_{\mathrm{res}}, 2\theta_{\mathrm{res}}, \ldots, \theta_{\max}\}$, where $\theta_{\min} = -10°$,$\theta_{\max} = 10°$ and the resolution of the discretezation is $\theta_{\mathrm{res}} = 0.5°$.

4. ADAPTATION OF THE TRANSITION PROBABILITIES

Characterizing the driving situation relying solely on historical data provides a good estimation of how the EV moves in the long term. However, the way a driver behaves might change depending on the traffic situation, the time of the day, the mood or the road condition. Because of this, a more proper prediction scheme requires predicting the driving load under an adaptive framework. This is achieved by updating the transition probabilities of $\boldsymbol{\Phi}^{va}$ and $\boldsymbol{\Phi}^{\theta}$ as new information about the driving situation becomes available. This allows to capture the *non-homogeneity* of the Markov process, which might be introduced by changes in the driver behavior, the traffic situation or the driving scenario. To this aim we employ a Bayesian posterior probability approach to update the established transition probabilities between Markov states.

4.1. Bayes Inference for Markov Chains

The Bayes' theorem estimates the *posterior* probability distribution of a parameter ψ by relating a *likelihood* function obtained from a set of observations $\mathbf{x}$ and an assumed *prior* probability distribution of the parameter. The update is computed by

$$p(\psi|\mathbf{x}) = \frac{\boldsymbol{\mathcal{L}}(\psi|\mathbf{x})\, p(\psi)}{\int_{\Psi} \boldsymbol{\mathcal{L}}(\psi|\mathbf{x})\, p(\psi)\, \mathrm{d}\psi}, \tag{20}$$

where $\boldsymbol{\mathcal{L}}(\psi|\mathbf{x})$ is the likelihood of the observed data, $p(\psi)$ is the prior probability distribution of ψ, $p(\psi|\mathbf{x})$ is the posterior probability distribution and Ψ represents the parameter space. The factor $\int_{\Psi} \boldsymbol{\mathcal{L}}(\psi|\mathbf{x})\, p(\psi)\, \mathrm{d}\psi$ is a normalization factor of $p(\psi|\mathbf{x})$. Eq. (20) can be expressed in terms of a normalized likelihood as follows

$$p(\psi|\mathbf{x}) \propto \boldsymbol{\mathcal{L}}(\psi|\mathbf{x})\, p(\psi). \tag{21}$$

As formulated in Eq. (21), applying the Bayes' theorem for updating a transition probability $\pi_{i,j}$, either of $\boldsymbol{\Phi}^{va}$ or of $\boldsymbol{\Phi}^{\theta}$,

requires a likelihood function for the new observed information and an assumption about prior distribution of $\pi_{i,j}$ on each row of the correspondent TPM. The forthcoming explanation deals with the theoretical foundations for updating any transition probability $\pi_{i,j}$ belonging to the mixture $\boldsymbol{\pi}_i = [\pi_{i,1}, \pi_{i,2}, \dots \pi_{i,j}, \dots, \pi_{i,m}]$, i.e., to the i^{th} row of $\boldsymbol{\Phi}$ in Eq. (9). The application of this method for updating $\boldsymbol{\Phi}^{va}$ or $\boldsymbol{\Phi}^{\theta}$ succeeds in a similar fashion.

4.1.1. Likelihood Function

Let the random variable q, representing a transition between two Markov states, to follow a multinomial distribution. The probability distribution of q can be parametrized by a vector $\boldsymbol{\pi}_i$, where $\pi_{i,j} = p\,(q_i \rightarrow q_j) = p\,(q_{i,j})$ is the probability of a transition from state i to state j, as it was already stated by Eq. (10). Then, the likelihood of a sequence of new transitions $\boldsymbol{\mathcal{Q}} = \{q_1, q_2, ..., q_n\}$ is given by

$$\boldsymbol{\mathcal{L}}\,(\boldsymbol{\pi}_i|\boldsymbol{\mathcal{Q}}) = \prod_{j=1}^{n} \pi_{i,j}^{\beta_{i,j}}, \tag{22}$$

where $\beta_{i,j}$ is the number of times a transition $q_i \rightarrow q_j$ occurs in $\boldsymbol{\mathcal{Q}}$. For the sake of convenience we express $\beta_{i,j} = \sum \delta_{i,j}$, where $\delta_{i,j} = 1$ if $q_i \rightarrow q_j$ occurs and $\delta_{i,j} = 0$, otherwise.

4.1.2. Prior Distribution

In the context of Markov chains, the task of the prior is to specify an assumption about the probability distribution of the i^{th} row $\boldsymbol{\pi}_i$ of $\boldsymbol{\Phi}$. Accordingly, it is necessary to find as many prior distributions as the number of Markov states. Updating the transition probabilities under a Bayesian approach works with any kind of prior. However, since we consider the arbitrary set of new transitions $\boldsymbol{\mathcal{Q}}$ to be multinomial distributed, it is mathematically convenient to use a *conjugate prior*. The use conjugate priors offers the advantage that the posterior distribution has the same functional form of the prior. The conjugate prior of the multinomial distribution is the Dirichlet distribution (Strelioff, Crutchfield, & Hübler, 2007). Thus, assuming the transition probabilities of a row from $\boldsymbol{\Phi}$ to be Dirichlet distributed leads to

$$p\,(\boldsymbol{\pi}_i|\alpha_{i,1}, \alpha_{i,2}, ..., \alpha_{i,m}) = \frac{\Gamma\left(\sum_{j=1}^{m} \alpha_{i,j}\right)}{\prod_{j=1}^{m} \Gamma\,(\alpha_{i,j})} \prod_{j=1}^{m} \pi_{i,j}^{\alpha_{i,j}-1}, \tag{23}$$

where the hyperparameter $\alpha_{i,j}$ can be understood as a virtual count of occurrences of $q_i \rightarrow q_j$ before considering new observations. Large values of $\alpha_{i,j}$ reflect strong prior knowledge about the distributions of the transition probabilities and small values of correspond to ignorance. The parameter m stands for the number of hyperparameters that parametrize Eq. (23).

The choice of the Dirichlet distribution as the prior is a fairly intuitive way to explain the meaning of the transition probabilities in $\boldsymbol{\Phi}$. A transition probability $\pi_{i,j}$ as defined by Eq. (10), can be understood as the first moment of the Dirichlet distribution evaluated for $\pi_{i,j}$. That is,

$$E\,[\pi_{i,j}] = \pi_{i,j} = \frac{\alpha_{i,j}}{\alpha_0}, \tag{24}$$

where $\alpha_0 = \sum_i \alpha_i$ is the total number of occurrences of a transition starting from state i. The Dirichlet distribution satisfies the unit simplex requirement $\sum E\,[\pi_{i,j}] = 1$ and $0 \leq E\,[\pi_{i,j}] \leq 1$ complying in this way with the properties of a row $\boldsymbol{\pi}_i$ in $\boldsymbol{\Phi}$. Furthermore, the uncertainty of a transition probability can be computed by the second moment

$$Var\,[\pi_{i,j}] = \frac{\alpha_{i,j}\,(\alpha_0 - \alpha_{i,j})}{{\alpha_0}^2\,(\alpha_0 + 1)}. \tag{25}$$

In our approach the parameters of the Dirichlet prior distribution are obtained from the offline estimation through MLE of section 3.1.1. In the absence of prior knowledge about the hyperparameters of Eq. (23), i.e., if $\boldsymbol{\Phi} \rightarrow \{0\}$ a common approach is to assume all probabilities to be equal. This can be achieved by setting all $\alpha_{i,j} = 1$, which results in a uniform prior distribution with an expectation value given by $E\,[\pi_{i,j}] = {}^1\!/_M$, where M represents the size of the state space.

4.1.3. Posterior Distribution

Having a multinomial likelihood and a Dirichlet prior, the posterior distribution of $\boldsymbol{\pi}_i$ after observing a new sequence of transitions $\boldsymbol{\mathcal{Q}}$ can be found in a closed form by exploiting the conjugate property of the Dirichlet distribution and the multinomial distribution. Accordingly, the posterior is computed by

$$p\,(\boldsymbol{\pi}_i|\boldsymbol{\mathcal{Q}}, \alpha) \propto \boldsymbol{\mathcal{L}}\,(\boldsymbol{\pi}_i|\boldsymbol{\mathcal{Q}})\,p\,(\boldsymbol{\pi}_i|\alpha) = \prod_{j=1}^{m} \pi_{i,j}^{\alpha_{i,j}+\beta_{i,j}-1}. \tag{26}$$

The posterior is computed on receipt of new observations. Considering the fact that in our system just one transition can occur per time step, we can set $\beta_{i,j} = \delta_{i,j}$. Accordingly, the set of hyperparameter α_i can be recursively updated by setting $\alpha_{i,k+1} = \alpha_{i,k} + 1$ if $q_i \rightarrow q_j$ or $\alpha_{i,k+1} = \alpha_{i,k}$, otherwise. By employing this Bayesian scheme the updated mean $E\,[\pi_{i,j}]_{k+1}$ and variance $Var\,[\pi_{i,j}]_{k+1}$ of each element in $\boldsymbol{\pi}_i$ can be computed with the help of Eq. (24) and Eq. (25). As it can be seen, the posterior computed by Eq. (26) keeps the information regarding all transitions occurred up to time step k.

Thus, depending on the values of the hyperparameters, many new observations might be needed in order to converge with the new Markov process. This is inconvenient in our application, since a slow adaptation of transition probabilities would

cause the characterization of the most up to date driving situation to fail. Because of this, it would be desirable to find a recursion for both $E\left[\pi_{i,j}\right]_k$ and $Var\left[\pi_{i,j}\right]_k$ without needing to deal with any prior knowledge about the hyperparameters and that can be carried such that the influence of older transitions in the computation of the posterior is progressively faded while keeping the underlying idea of an a Bayesian update.

The aforementioned recursion is achieved by means of the discounted mean-variance estimator shown in (Bertuccelli & How, 2008) such that

$$E\left[\pi_{i,j}\right]_{k+1} = E\left[\pi_{i,j}\right]_k + \frac{Var\left[\pi_{i,j}\right]_k \left(\delta_{i,j} - E\left[\pi_{i,j}\right]_k\right)}{\lambda_k E\left[\pi_{i,j}\right]_k \left(1 - E\left[\pi_{i,j}\right]_k\right)}, \tag{27}$$

and

$$\mathrm{Var}\left[\pi_{i,j}\right]_{k+1} = \frac{\mathrm{Var}\left[\pi_{i,j}\right]_k E\left[\pi_{i,j}\right]_{k+1}\left(1 - E\left[\pi_{i,j}\right]_{k+1}\right)}{\lambda_k E\left[\pi_{i,j}\right]_k \left(1 - E\left[\pi_{i,j}\right]_k\right) + \mathrm{Var}\left[\pi_{i,j}\right]_k}, \tag{28}$$

where $\lambda_k < 1$ is a factor used to scale the variance at each iteration, which makes the estimation to be more responsive to new observations. (Bertuccelli & How, 2008) shows that convergence to the true moments is achieved if $\lim_{k\to\infty} \lambda_k = 1$. We thus consider using in this work a decaying factor $\lambda_k = 1 - \frac{\lambda}{k}$, where $0 < \lambda < 1$ and k denotes the time step.

5. DRIVING LOAD PREDICTION

The prediction of the driving load proceeds as presented in Algorithm 1. At every time step measurements of the input space, i.e., $\mathbf{u_k} = \begin{bmatrix} v_k & a_k & \theta_k \end{bmatrix}^T$ are acquired and processed in order to determine the indices s, i and h, which are used to allocate the measurements in the correspondent position of the Markov state space.

First, the information about the speed and the acceleration is updated. To this aim the index s determines the transition probability matrix $\mathbf{\Phi}^{v_s a}$ to be updated. The index i is used to find the row within the matrix, which contains the information about the last observed transition. Having located the row containing the transition of interest, all transition probabilities $\pi_{i,j}^{v_s a} \in \boldsymbol{\pi}_i^{v_s a}$ are simultaneously updated by means of Eqs. (27) and (28), ensuring in this way that the entire row sums up to one. Analogous, the index h is used to determine the row of $\mathbf{\Phi}^{\theta}$ to be updated. The update of the slope information succeeds similarly to the procedure previously presented.

At every prediction time k_p the driving load is predicted for a given horizon length h_l. A prediction consists of synthetically generating one profile for the speed/acceleration and one for the slope via Markov chains. The generated profiles are then processed by the EV model in order to compute the driving load.

The generation of the speed/acceleration profile starts by randomly drawing from $\boldsymbol{\pi}_i^{v_s a}$ a sample a_j for the next state a_{k+1} according to the current values of speed v_k and acceleration a_k. To this aim the *inverse transformation method* is employed, since $\boldsymbol{\pi}_i^{v_s a}$ represents a discrete probability distribution. If no information about the distribution of a_{k+1} is available, i.e., if $\boldsymbol{\pi}_i^{v_s a} \to \{0\}$, then a_j is randomly sampled from $Beta\left(\alpha\left(v_s, a_i\right), \beta\left(v_s, a_i\right), a_{\min}, a_{\max}\right)$, where $\alpha\left(v_s, a_i\right)$ and $\beta\left(v_s, a_i\right)$ are given by Eq. (17) and Eq. (18), respectively. This step ensures a complete generation of the profile regardless of the lack of information about the distribuiton of a_{k+1}.

Algorithm 1 Driving Load Prediction

Require: $\mathbf{\Phi}^{va}, \mathbf{\Phi}^{\alpha}, \mathbf{u}_k, \mathbf{\Omega}, \Delta t, h_l$
Ensure: $\left\{P_{ele,k_p}, P_{ele,k_p+1}, ..., P_{ele,k_p+h_l}\right\}$
  Initialize:
  Determine the indices s, i and h for the current speed, acceleration and slope.
  $v_s \leftarrow v_k$, $a_i \leftarrow a_k$, $\theta_h \leftarrow \theta_k$
  Update $\mathbf{\Phi}^{v_s a}$ and $\mathbf{\Phi}^{\theta}$ ▷ Use Eqs. (27) and (28) to:
  Compute $E\left[\pi_{i,j}^{v_s a}\right]$ and $Var\left[\pi_{i,j}^{v_s a}\right]$ for all $\pi_{i,j}^{v_s a} \in \boldsymbol{\pi}_i^{v_s a}$
  Compute $E\left[\pi_{i,j}^{\theta}\right]$ and $Var\left[\pi_{i,j}^{\theta}\right]$ for all $\pi_{i,j}^{\theta} \in \boldsymbol{\pi}_i^{\theta}$
  if $k = k_p$ **then**
    for $l = 1$ **to** h_l **do**
      Randomly draw a_j for the next state according to:
      if $\boldsymbol{\pi}_i^{v_s a} \to \{0\}$ **then**
        $Beta\left(\alpha\left(v_s, a_i\right), \beta\left(v_s, a_i\right), a_{\min}, a_{\max}\right)$
      else
        $\mathbf{\Phi}^{v_s a}\left(a_{k+1} = a_j | a_k = a_i, v_k = v_s\right)$
      end if
      $a_{k+1} \leftarrow a_j$
      Compute v_{k+1} ▷ Use Eq. (29)
      $\mathbf{u}_{k+1}^{va} \leftarrow \begin{bmatrix} v_{k+1} & a_{k+1} \end{bmatrix}$
      Randomly draw θ_j for the next state according to:
      $\mathbf{\Phi}^{\theta}\left(\theta_{k+1} = \theta_j | \theta_k = \theta_h\right)$
      $u_{k+1}^{\theta} \leftarrow \theta_j$
      Set the input for the next time step
      $\mathbf{u}_{k+1} \leftarrow \begin{bmatrix} \mathbf{u}_{k+1}^{va} & u_{k+1}^{\theta} \end{bmatrix}^T$
      Compute the power demand for the current time step
      $P_{ele,k} = f\left(\mathbf{u}_k, \mathbf{\Omega}\right)$ ▷ Use Eqs. (2), (3) and (4)
      $k \leftarrow k + 1$
    end for
  end if

Contrary to other methods for generating synthetic driving profiles (T. Lee & Filipi, 2011), our approach compute the value of the speed in the next speed instead of randomly sample it. Here v_{k+1} is given by

$$v_{k+1} = v_k + a_k \Delta t, \tag{29}$$

where Δt denotes the time step size used in the generation of the profile. Our approach is efficient, since computing Eq. (29) for obtaining the speed is more efficient than sampling it from any discrete distribution. After obtaining the values of a_{k+1} and v_{k+1}, the next step is to draw a sample θ_j for the next time step according to the value of θ_k.

Having predicted $\mathbf{u}_{k+1} = \begin{bmatrix} v_{k+1} & a_{k+1} & \theta_{k+1} \end{bmatrix}^T$ the electrical power demand is computed by means of Eqs. (2), (3) and (4). To this aim the set $\mathbf{\Omega}$ containing the parameters of the EV model is needed. This procedure is repeated iteratively until the desired horizon length h_l of the prediction is reached.

6. RESULTS AND DISCUSSIONS

This section first introduces the experimental system used for validating the prediction of the driving load. Afterwards, the assumption regarding the Markovianity of the input variables is validated through simulation. Finally, a series of experimental case studies used to illustrate the applicability of our approach in different driving situations is presented.

6.1. Experimental Setup

The EV used as experimental platform for gathering the data and for testing the proposed approach is propelled by a 80 kW and 280 Nm synchronous electric motor mounted in the front axle and is powered by a 24 KWh Li-ion battery pack rated to deliver up to 90 kW. The vehicle is equipped with a GPS used to gather information about the speed and the acceleration of the vehicle and the height profile of the road. A system for measuring the voltage and the current of the motor is also integrated. A data acquisition system is used to synchronize the information delivered by these two systems.

EV Model Parameters

Parameter	Value
A	2.29 m^2
c_w	0.28
m	1520 kg
K_r	0.7
$T_{m,\max}$	280 Nm
$P_{ele,\max}$	80 kW
r_{tire}	0.3 m
ρ_{air}	1.226 $\mathrm{kg/m}^3$
g	9.81 $\mathrm{m/s}^2$

Table 2. Parameters used for computing the driving load.

Table 2 shows the constant parameters used to compute the driving load. It is worth noting that both m and K_r have to be identified from real data, since they depend on the cargo weight (given by the driver) and on the road condition, respectively. In this work both parameters are identified offline by fitting, in the least-square sense, the measured power consumption for a given trip with to power demand computed by the model for the same trip.

6.2. Validating the Markov Assumption

In this work a set historical drive cycles together with a set of height profiles is employed. This information is used for estimating the transition probabilities of $\mathbf{\Phi}^{va}$ and $\mathbf{\Phi}^{\theta}$ by MLE. Then, $\mathbf{\Phi}^{va}$ is approximated with the methodology presented in section 3.1.2 for those regions with unavailable data. Due to the wide spectrum of driving situations covered by the chosen driving data, the estimated TPMs offer a proper starting point for predicting the driving load under different driving scenarios.

To validate the assumption about the Markovianity of the input variables a set of synthetic profiles is generated as shown in Algorithm 1, with the only difference being that the update step is skipped. This allows us to model the input variables as a *homogeneous* Markov process, which suffices at this stage of the validation. The simulated profiles are then compared with the data used for training the TMPs in order to see if the distribution of the synthetic input variables correspond to that of the original data. In this work we compute the probability distribution of the data by means of kernel density estimation. As it can be seen in Fig. 9, the distribution of the generated profiles accurately describes the original data. It is important to notice that the probability distribution of the speed is left truncated, due to only non-negative speeds are considered.

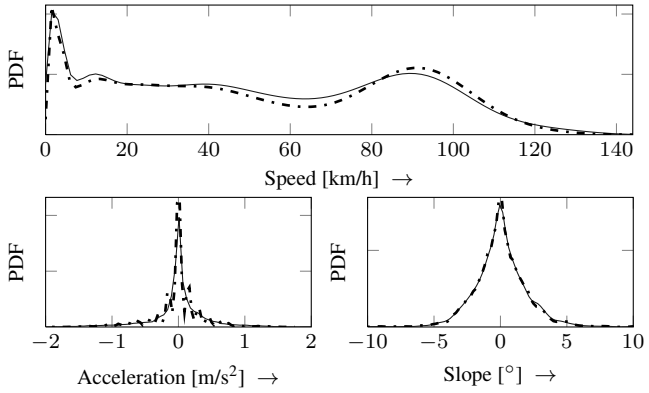

Figure 9. Probability distribution of the measured and simulated speed (top), the acceleration (bottom-left) and the slope (bottom-right). The solid and the dashed lines correspond to the measurements and to the model, respectively.

Furthermore, it is of interest to investigate the impact computing the speed with Eq. (29) instead of considering it part of the Markov chain. To this aim we employ the joint speed-acceleration frequency distribution (SAFD) depicted in Fig. 10. The SAFD offers a good overview of the driving situations exhibited by the driving data. As it can be appreciated, the simulated driving profiles successfully models the real driving data in low-speed regions. However, the simulated data lies very tight in regions above 80 km/h. This is due to the drive cycles chosen to estimate $\mathbf{\Phi}^{va}$ mainly describe driving situations in the city and rural areas. The usability of the methodology presented in section 3.1.2 can be proved by simulating driving data and by finding out the percentage of data generated by using a Beta distribution. From 500 000 s of simulated data a total of 4.7% was identified to be generated using this methodology.

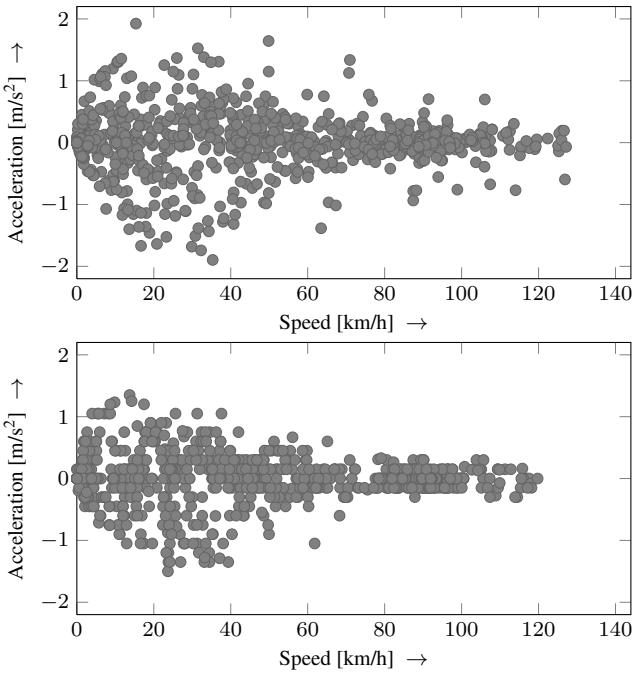

Figure 10. Joint frequency distribution of the measured (top) and simulated (bottom) speed and acceleration profiles.

The power demand is computed by simulation using both the training and the simulated input variables together with the parameters shown in Table 2 . Fig. 11 depicts the distribution of the power demand. As it can be seen, the proposed approach accurately models the power demand of the EV, specially important being the region with negative values, i.e., the distribution of power recovered through the regenerative braking system.

The auto-covariance function (ACF) confirms that the power demand of the EV can be predicted using a model-approach with input variables modeled as Markov processes.

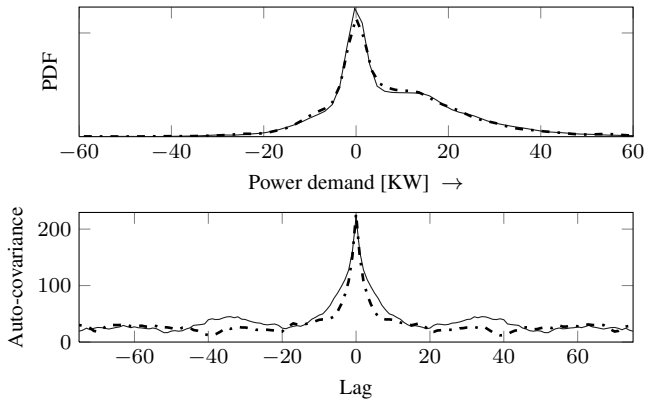

Figure 11. Probability distribution (top) and ACF (bottom) of the measured and simulated power demand. The solid and the dashed lines correspond to the measurements and to the model, respectively.

6.3. Experimental Case Studies

The proposed approach for adaptively predicting the driving load is validated through a series of trips. Each trip takes place along a different road and under a different driving situation. Three driving situations are tested, namely driving in the city, in rural areas and driving in a combination of highway and city. All trips start with the $\mathbf{\Phi}^{va}$ and $\mathbf{\Phi}^{\theta}$ estimated in section 6.2, so that no previous information about the driver behavior or the driving scenario is available. This allows investigating the adaptability of the TPMs for the different driving situations.

6.3.1. Scenario 1: City

The speed and the slope profile of the first trip are shown in Fig. 12. Here the EV travels 9.17 km in approximately 20 minutes. The speed profile exhibits the common behavior of a vehicle traveling in a city with many stops and a maximum speed of approximately 50 km/h.

Fig. 13 shows the probability distribution of the predicted input variables together with the computed power demand. The prediction takes place at $k_p = 600$ s, that is 10 minutes after beginning the trip and the horizon length of the prediction is $h_l = 600$ s. As it can be seen, the shape of PDF of the speed resembles the real distribution. In the same manner the PDF of the distribution fits the measured data. The difference in the distribution of the predicted slope profile with the real measurements is due to the discretization resolution used in the Markov chain.

This causes the predicted slope to be more focused in some regions, e.g. $0°$, in comparison to the real measurements where the data is more widespread. Despite the difference in the slope distribution, the PDF of the electrical power succeeds to describe the distribution for both demanded and recovered power.

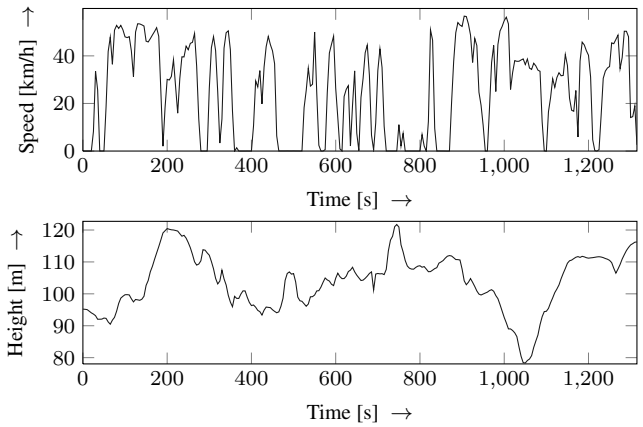

Figure 12. Driving situation representing a trip in the city.

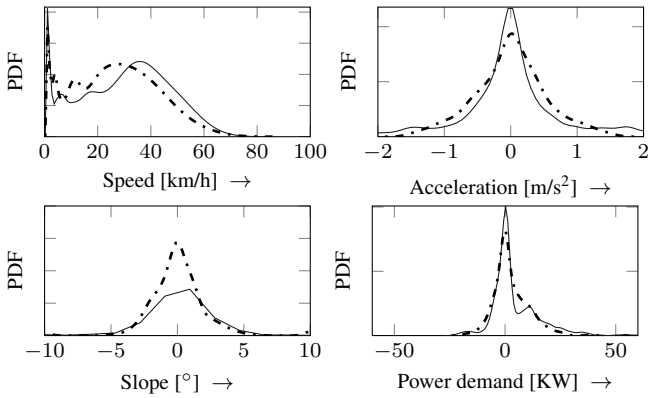

Figure 13. Snapshot at $k_p = 600$ s of the probability distribution of the predicted input variables and the power demand for $h_l = 600$ s in the city scenario. The solid and the dashed lines correspond to the measurements and to the model, respectively.

6.3.2. Scenario 2: Rural Areas

The second trip is depicted in Fig. 14. In this trip the EV travels 17.03 Km along a rural road. The approximate duration of the entire trip is 30 minutes. This driving scenario is characterized by transition between zones with maximum speed of 50 km/h and 70 km/h. The height profile remains almost constant during the trip, with exception of the last 5 minutes where the slope of the road slightly increases. The probability distribution of the predicted input variables and the computed power demand is presented in Fig. 15. The distributions shown are the result of a prediction carried out 5 minutes after the beginning of the trip. i.e., $k_p = 300$ s. In this case the $h_l = 1\ 500$ s. As it can be noticed, the distribution of the predicted speed presents a region of high probability near to the zero speed. This is the result of the large stop of approximately 100 s occurred at time step $k = 400$ s. Similarly to results shown in the previous case, the distribution of the power demand successfully captures the uncertainty of the prediction.

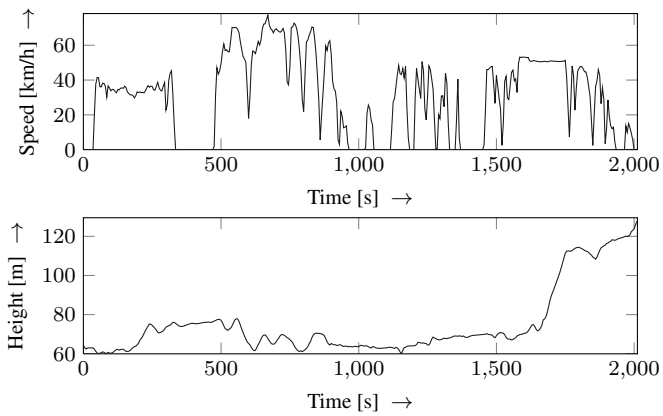

Figure 14. Driving situation representing a trip in rural areas.

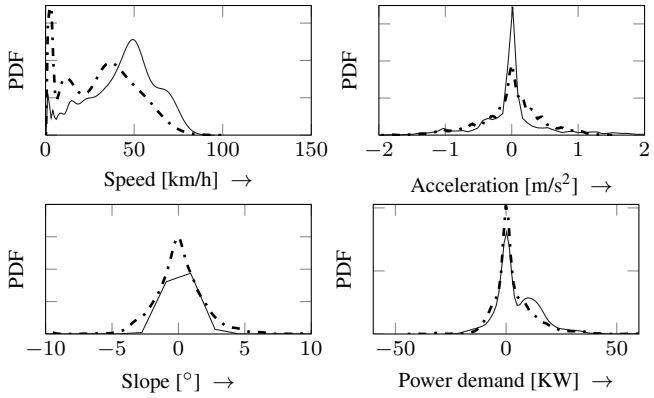

Figure 15. Snapshot at $k_p = 300$ s of the probability distribution of the predicted input variables and the power demand for $h_l = 1\ 500$ s in the rural scenario. The solid and the dashed lines correspond to the measurements and to the model, respectively.

6.3.3. Scenario 3: Highway-City

The last experimental case study illustrates the flexibility of our approach. Both the speed and the high profile are shown in Fig. 16.

The purpose of this experiment is to test the ability to adapt the driving load prediction to the change in the driving situation. To this aim the EV travels 75.28 Km on the highway followed by 20.3 Km in the city. The driving behavior on the highway is characterized by a mean speed above 100 km/h and by very few stops. A very important feature of this driving scenario is the large increment on the height profile in one segment of the road. In this case two prediction were carried out, each of them with a horizon length $h_l = 1\ 500$ s.

Fig. 17 shows the probability distribution of the predicted input variables and the power demand for the first prediction at $k_p = 1\ 800$ s. As it can be seen the PDF of the predicted speed differs from the real distribution, in that the region with low speed is almost neglected. This is due to the segment of city contained withing the horizon length of the prediction is not taken into consideration. This causes the power demand to be slightly overestimated.

At $k_p = 3\ 600$ s a new prediction is carried out. In this case the EV travels in a city driving scenario. As it can be seen in Fig. 18 the PDF of the predicted speed profile seems to converge to the real distribution. Accordingly, the distribution of the predicted driving load resembles very accurately the shape of the real distribution. This shows that the proposed approach succeeds in predicting the driving load even if remarkable changes in the driving situation occur.

7. CONCLUSIONS AND FUTURE WORK

In this work a methodology for predicting the driving load of an EV in uncertain environments is presented. The pre-

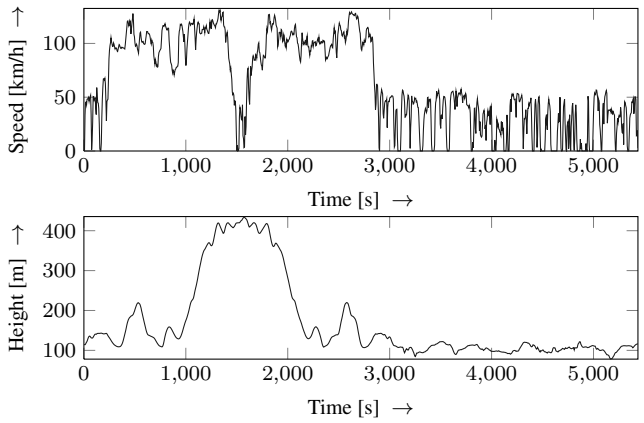

Figure 16. Driving situation representing a trip combining highway and city segments.

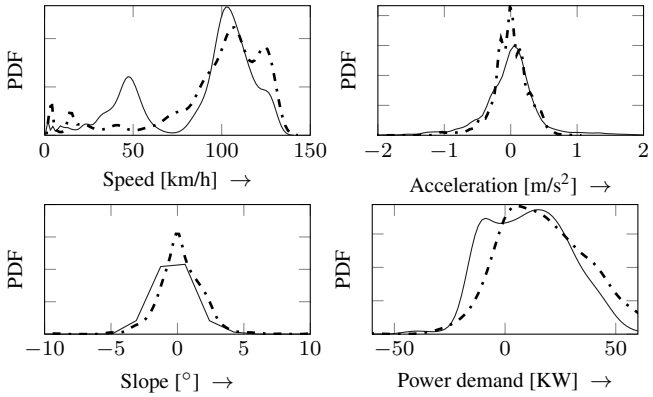

Figure 17. Snapshot at $k_p = 1\ 800$ s of the probability distribution of the predicted input variables and the power demand for $h_l = 1\ 500$ s in the combined highway-city scenario. The solid and the dashed lines correspond to the measurements and to the model, respectively.

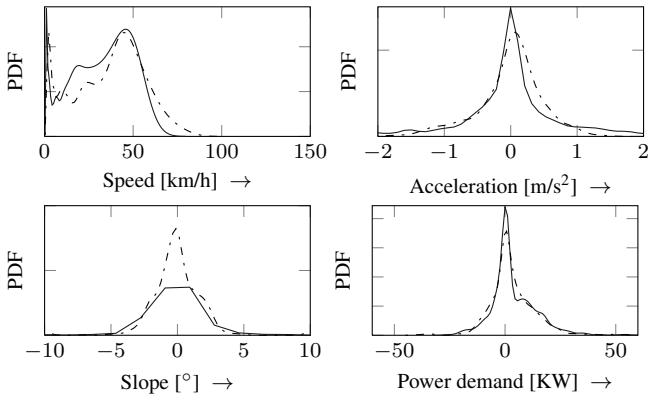

Figure 18. Snapshot at $k_p = 3\ 600$ s of the probability distribution of the predicted input variables and the power demand for $h_l = 1\ 500$ s in the combined highway-city scenario. The solid and the dashed lines correspond to the measurements and to the model, respectively.

diction takes place under a model-based approach, in which the input variables of an EV model, used to describe the driving situation, are modeled as first order discrete-time Markov processes. The transition probabilities between Markov states are first estimated offline from historical driving data via maximum likelihood estimation. Furthermore, an approach for estimating transition probabilities in the presence of sparse data is introduced. In order to account for most up to date driving situations, road conditions and driving behaviors in the driving load prediction, the transition probabilities are recursively updated via Bayesian inference.

The validity of the proposed methodology is illustrated through simulation and by means of a series of experimental cases of study. The obtained results suggest, that the driving load can be successfully predicted with our approach regardless of the driving environment. Nevertheless, it has been realized that by abrupt changes in the driving situation within a trip, the time the transition probabilities take to converge to the new driving situation can become large.

An aspect we aim to investigate in the future is therefore to model the transition between driving situations as a Markov jump process. In this way, it would be possible to choose different TPMs according to some stochastic process describing the change between driving situations.

ACKNOWLEDGMENT

The funding for this work was provided by the EU and the federal state of North Rhine-Westphalia (NRW) in frame of the Ziel2 project "Technology and test platform for a competence center for interoperable electromobility, infrastructure and networks" (TIE-IN).

REFERENCES

Abourizk, S. M., Halpin, D. W., & Wilson, J. R. (1994). Fitting Beta Distributions Based on Sample Data. *Journal of Construction Engineering and Management*, *120*(2), 288-305.

Bertuccelli, L., & How, J. (2008). Estimation of non-stationary markov chain transition models. In *Decision and Control (CDC), IEEE conference on* (p. 55-60).

Guzzella, L., & Sciarretta, A. (Eds.). (2005). *Vehicle propulsion systems: Introduction to modeling and optimization*. Springer Verlag, Heildelberg.

Johannesson, L. (2005). *Development of a time invariant stochastic model of a transport mission* (Tech. Rep.).

Johannesson, L., Asbogard, M., & Egardt, B. (2007). Assessing the Potential of Predictive Control for Hybrid Vehicle Powertrains Using Stochastic Dynamic Programming. In *Intelligent transportation systems, IEEE transactions on* (Vol. 8, p. 71-83).

Kim, E., Lee, J. L., & Shin, K. G. (2013). Real-time pre-

diction of battery power requirements for electric vehicles. In *ACM/IEEE 4th international conference on cyber-physical systems (ICCPS 13)*.

Lee, T., & Filipi, Z. (2011). Representative real-world driving cycles in Midwestern US. In *Les rencontres scientifiques d'lFP energies nouvelles - RHEVE 2011*.

Lee, T. C., Judge, G. G., & Zellner, A. (Eds.). (1970). *Estimating the parameters of the markov probability model from aggregate time series data.* North-Holland, 2nd edition.

Oliva, J. A., Weihrauch, C., & Bertram, T. (2013). A model-based approach for predicting the remaining driving range in electric vehicles. In *Annual conference of the prognostics and health management society 2013.* (p. 438-448).

Strelioff, C. C., Crutchfield, J. P., & Hübler, A. W. (2007). Inferring Markov Chains: Bayesian estimation, model comparison, entropy rate, and out-of-class modeling. *Physical Review E (Statistical, Nonlinear, and Soft Matter Physics)*, *76*(1).

Wang, Z., Xu, G., Li, W., & Xu, Y. (2007). Driving load forecasting using cascade neural networks. In *Advances in neural networks ISNN 2007* (Vol. 4493, p. 988-997). Springer Berlin Heidelberg.

Yang, J., Huang, X., Tan, Y., & He, X. (2008). Forecast of driving load of hybrid electric vehicles by using discrete cosine transform and Support Vector Machine. In *Neural networks, IEEE International Joint Conference on* (p. 2227-2234).

BIOGRAPHIES

Javier A. Oliva received his B.S. degree in Mechanical Engineering from the University Landivar in Guatemala in 2006 and his M.S. degree in Automation and Robotics from the Technische Universität Dortmund in 2010. His research interests include probabilistic methods, diagnosis and prognostics applied to electric vehicles. He is currently working as researcher at the Institute of Control Theory and Systems Engineering from the TU Dortmund in the area of driver assistance systems for electric vehicles.

Torsten Bertram is Professor at the Technische Universität Dortmund and he directs the Institute of Control Theory and Systems Engineering. He has carried out applied research in the areas of drive systems, service robotics and development methodology.